Proceedings of 3rd Asian Conference on Mixing
October 19-22, 2010, Jeju, Korea

Paper No. ACOM2010-xxxxx

PRACTICAL DATA OF THE HEAT TRANSFER COEFFICIENT AT THE INSIDE WALL OF AN AGITATED VESSEL

Zauyah Zamzam*[1], Hisayuki Kanamori[1], Takashi Yamamoto[1] and Yoshikazu Kato[1]
[1]Mixing Technology Laboratory
Satake Chemical Equipment MFG. LTD., Saitama, Japan 335-0021
* E-mail: zauyah@satake.co.jp

ABSTRACT

In this study, a new method presented by Kanamori *et al.* was practically used to determine the heat transfer coefficient at the inside wall of an agitated vessel in the high mixing Reynolds number region. The impellers used are a 3-bladed propeller, a 4-bladed pitched paddle and a 6-bladed flat turbine of the conventional impellers and Satake Supermix MR210 of the large impeller. The characteristics of each impeller were made clear based on the experimental results by investigated the effects of the impeller speed, baffling conditions (2-baffled and non-baffled) and the impeller positions on the heat transfer coefficient.

Moreover, a new information concerning about the relations of the flow pattern and flow velocity distribution on the heat transfer coefficient was also clarified. Finally, it is expected that the new heat transfer coefficient measuring method present the useful information for a new design of mixing device.

INTRODUCTION

Heat transfer in agitated vessels is a common industrial practice that has been researched extensively. Heat transfer operation plays important roles on the mixing device such as:
1. Heat elimination on the chemical reaction.
2. Fluid temperature control on the crystallization.
3. Fluid temperature rising on the dissolution process.
and others.

Generally, the accuracy of the temperature measurement in the range of high Reynolds numbers may depend on how to set the thermocouple. Rigorous methods of temperature measurement were investigated. Traditionally, many workers employed the extrapolation method by inserting two or more thermocouples inside the vessel wall [2], [4], [5] and setting the thermocouple on the surface of the vessel wall which is trenched inside the channel [5].

The main purpose of this paper is to presents the practical data of the heat transfer coefficient at the inside wall of an agitated vessel by using a new heat transfer coefficient measuring method presented by Kanamori *et al*. This new measuring method is simple and is expected to be more practical and more precise that enables to provide an effective measurement application for the mixing device in the future.

Additionally, this work is also to make clear the relationship between the heat transfer coefficient distributions with the flow velocity distribution and the flow pattern inside agitated vessels. In order to achieve these purpose:
1. The heat transfer coefficient distribution (h distribution) is determined by using a new measuring method experimentally.
2. The relationship between the h distribution and the flow velocity is investigated.
3. The effect of the flow pattern inside agitated vessels on the h distribution at the vessel wall is identified.

in a wide range of experimental conditions and impeller designs.

EXPERIMENTAL METHODS AND DEVICES

1.1 *Experimental Devices*

Fig. 1 is a schematic diagram of the experimental device. The vessel diameter was Φ250mm and the height of the liquid in the vessel was 325mm. Experiments were carried out under a condition of steady state heat transfer in which steam (107°C) was fed into the jacket and overflowed and water (50°C, 6L/min.) was fed inside the vessel and overflowed. The volume of the water inside the vessel was kept constant. There were five measuring points at the vicinity of the vessel wall, as shown in Fig. 1. The heat transfer coefficients were measured at these five measuring points. A summary of the experimental conditions; baffling conditions, impeller positions and impeller speed are shown in Table 1.

The flow velocity distribution and the flow pattern inside agitated vessels were measured by using the experimental device shown in Fig. 2. The vessel was made of a transparent acrylic resin with a diameter of Φ240mm. Water was used as an experimental medium inside the vessel. Particle tracers for L.D.V. (Laser Doppler Velocimetry) and P.T.V. (Particle Tracking Velocimetry) were Expancel and Nylon 12 in micro order, which are in spherical shapes. The density of these particle tracers are almost similar with the water used. For the light sheet, an Argon-ion laser was used.

In P.T.V. [1], [3] each particle tracers were tracked by using four time steps that later detected by using the tracking algorithm. High performance speed of CCD Camera (100f/s) was used to record multiple images of the moving particles. The P.T.V. measurement was set at (a) overall view : (240×270)mm, (b) vicinity to the vessel wall : (90×145)mm and (c) vessel bottom : (120×147)mm as shown in Fig. 3.

The flow velocity, V was evaluated by using the following Eq. (1):

$$V = [(V_z)^2+(V_\theta)^2]^{1/2} \qquad (1)$$

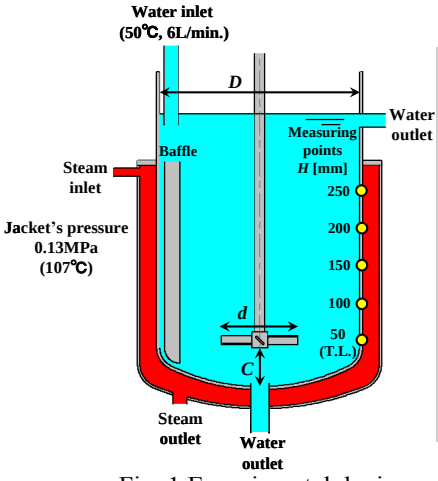

Fig. 1 Experimental device

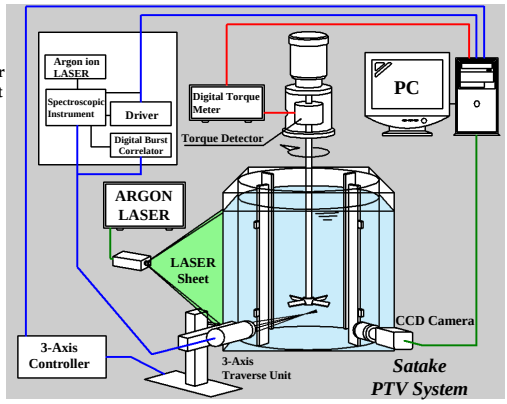

Fig. 2 P.T.V. and L.D.V. system

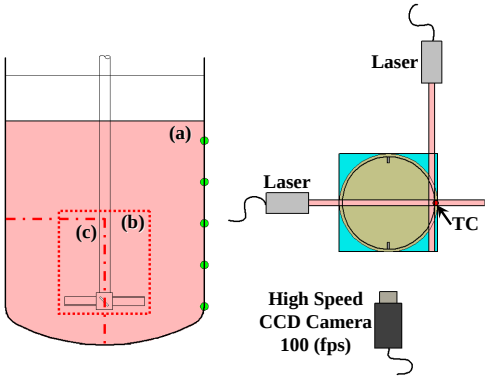

(i) Front View (ii) Upper View

Fig. 3 P.T.V. analysis cross-section

In the above equation, V_z and V_θ is the component of the axial and tangential velocity, respectively. The measuring points were 6mm from the vessel wall.

1.2 *Experimental Materials*

Besides the conventional impellers, Satake Supermix impeller of MR210 with Φ156mm in diameter and 264mm in height was also used as the representative of the large impeller. The clearance of the impeller and the vessel bottom was set at 5mm.

Three types of conventional impellers were used; 4-bladed pitched paddle (4PP), 3-bladed propeller (3P) and 6-bladed flat turbine (6FT) with Φ96mm in diameter.

Table 1 Experimental conditions

Baffling conditions	2-baffled Non-baffled
Impeller positions, *C*/*d* [-]	0.5 1.0 1.2
Impeller speed, *N* [min^{-1}]	120 180 240 300 360

RESULTS AND DISCUSSIONS

1. *Results discussions in 2-baffled agitated vessels*

1.1 *The effect of the impeller positions*

1.1.1 *Heat transfer coefficient distribution*

Figs. 4, 5 and 6 show the effect of the impeller positions on the heat transfer coefficient distribution (h distribution) in the axial direction at the vessel wall in 2-baffled agitated vessels for 3P, 4PP and 6FT, respectively. In the case of 3P and 4PP, the h distribution is the highest at the impeller position is located at 0.5 with the maximum h distribution is obtained at the tangential level (T.L.).

In contrary, the highest h distribution is obtained at the impeller position is located at 1.0 for 6FT, although there is a slightly declination at the T.L.

1.1.2 *Flow velocity distribution*

In order to clarify the relationship between h distribution and flow velocity, the flow velocity was measured by changing the impeller positions. Figs. 7, 8 and 9 show the results obtained for 3P, 4PP and 6FT, respectively. It is well understood that in the case of 3P and 4PP, the flow velocity is apparently highest at the impeller position is located at 0.5. Moreover, the flow velocity is also almost identical at the impeller positions are located at 1.0 and 1.2.

Regardless of the impeller positions, the flow velocity showed a slightly declination at the T.L. This may probably indicated that the main flow may occupied by the radian velocity than the tangential velocity at this point. However, the flow velocity is almost constant at the impeller position is located at 1.0 for 6FT. In contrary, wide range of flow velocity is obtained at the other impeller positions.

1.1.3 *Flow pattern*

In order to make clear on the effect of the flow pattern on the h distribution, the flow pattern is visualized by changing the impeller positions. Figs. 10 and 11 illustrate the flow pattern for 3P and 4PP at the impeller position is located at 0.5. It is clearly observed that a strong axial flow is discharged by the blades and strike the vessel wall with sharp angle at the T.L. for both impellers. This sharp angle is noticed to provide greater affect to the thermal boundary layer at the vessel wall. Subsequently, maximum h distribution is obtained at the T.L.

Fig. 12 illustrates the flow pattern for 6FT at the impeller position is located at 1.0. Two complete circulating zones are generated with the radial discharged flow by the blades strike the vessel wall with a sharp angle at the vessel bottom near to the T.L. Therefore, maximum h distribution is obtained at this point. However, since the impeller position is farther away from the vessel bottom, less flow attack to the vessel wall at the T.L. is considered to be the main factor contributed to the decreases in h distribution at this point.

1.2 *The effect of the impeller speed*

1.2.1 *Heat transfer coefficient distribution*

Figs. 13, 14, 15 and 16 display the effect of the impeller speed on the h distribution for 3P, 4PP, 6FT and MR210, respectively. It is well observed that h distribution is dependent on the impeller speed for these impellers. The h

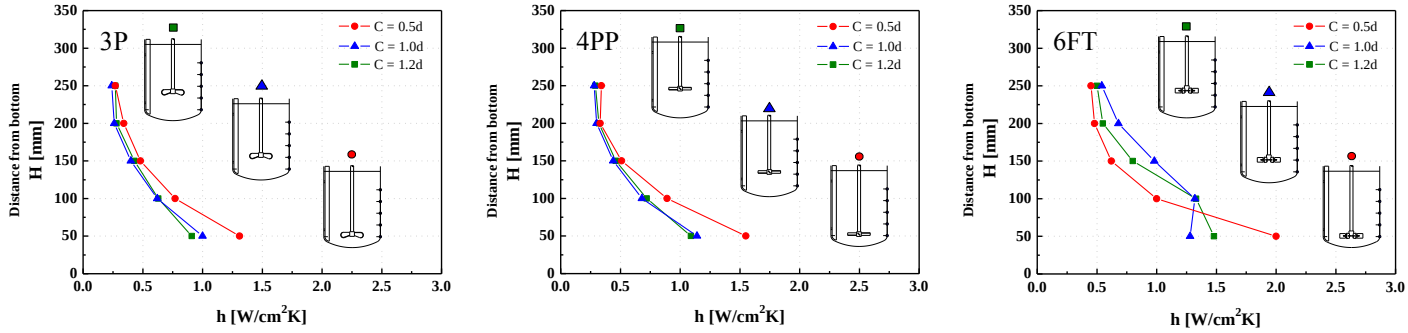

Figs. 4, 5, 6 H vs. h (from left: 3P, 4PP, 6FT) under the effect of impeller position

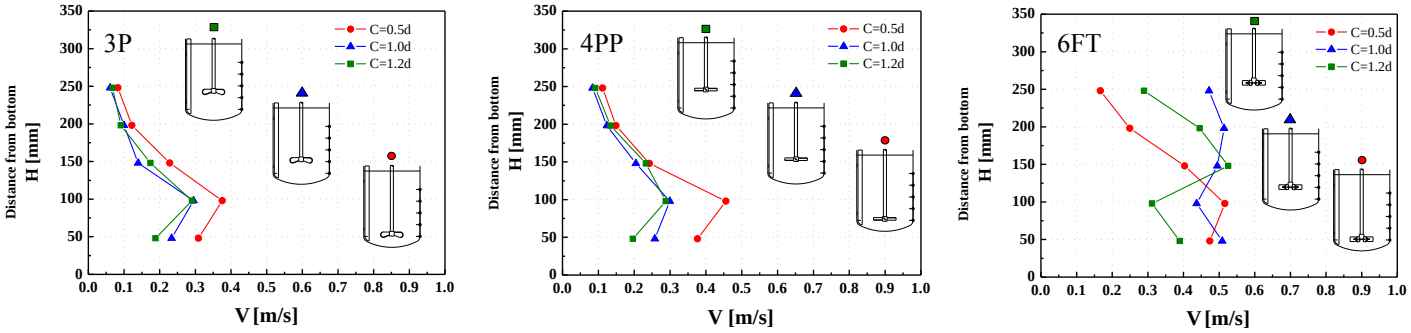

Figs. 7, 8, 9 H vs. V (from left: 3P, 4PP, 6FT) under the effect of the impeller position

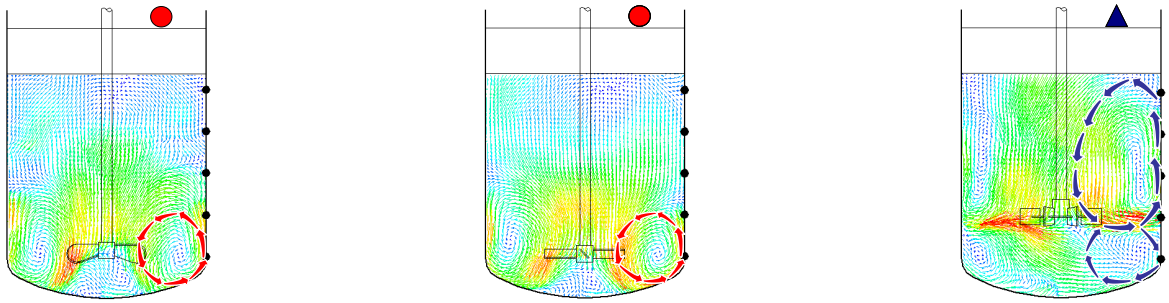

Figs. 10, 11, 12 Flow pattern (from left: 3P, 4PP, 6FT)

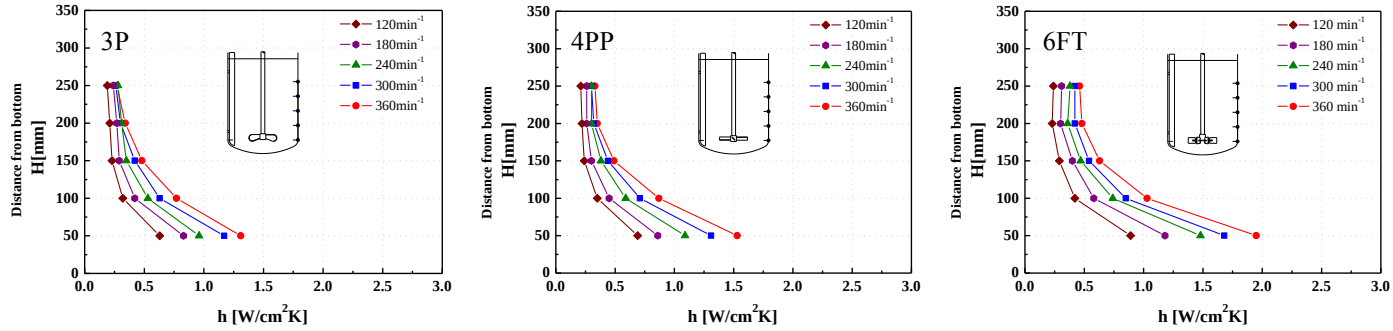

Figs. 13, 14, 15 H vs. h (from left: 3P, 4PP, 6FT) under the effect of impeller speed

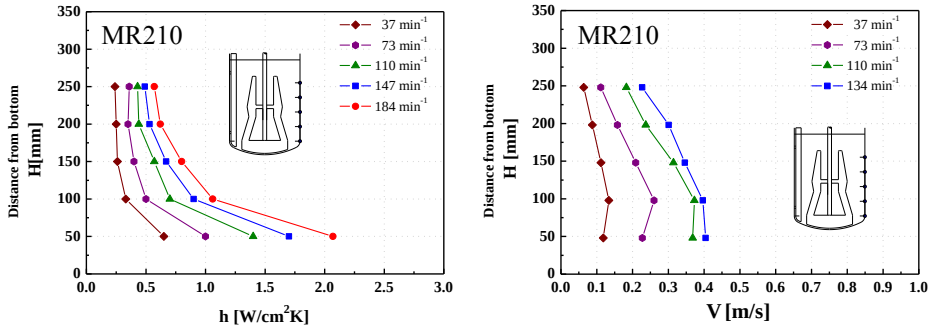

Fig. 16, 17 From left: H vs. h, H vs. V under the effect of impeller speed

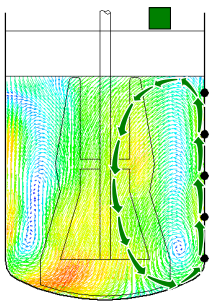

Fig. 18 Flow pattern of MR210 (C/d = 0.5)

distribution spreads wider as approaching to the T.L. and the maximum h distribution is obtained at the T.L. This indicated that the higher the impeller speed showed a good tendency to obtain higher h distribution.

1.2.2 *Flow velocity distribution*

The effect of the impeller speed on the flow velocity for MR210 is shown in Fig. 17. The flow velocity is increases as the impeller speed increased.

1.2.3 *Flow pattern*

The effect of the flow pattern on the h distribution is investigated for MR210, as shown in Fig. 18. For MR210, a large circulation flow is generated and the strong flow from the vessel bottom gets along the vessel wall closely. This flow characteristic of MR210 contributes to the constant flow velocity thoroughly in the agitated vessel.

Furthermore, a sharp angle flow strikes at the T.L. which exhibits greater affect to the thermal boundary layer thickness that provided maximum h distribution at the T.L.

1.3 *Comparative data at constant C/d and constant Pv*

1.3.1 *Heat transfer coefficient distribution*

Fig. 19 and 20 show the comparative results of 4PP and 6FT, 4PP and MR210 at Pv = 0.2 [kW/m^3] and C/d = 0.5 constant, respectively. The h distribution is almost similar at most of the measuring points except at the vessel bottom position near to the T.L., which the h distribution is greater for 4PP than 6FT.

Meanwhile, comparing to 4PP, the h distribution is almost constant for MR210. However, h distribution is increased profoundly at T.L. and vessel bottom position near to the T.L. for 4PP.

1.3.2 *Flow velocity distribution*

The flow velocity for 4PP and 6FT, 4PP and MR210 are shown in Fig. 21 and 22, respectively. From these results, it is well understood that the flow velocity is greater for 4PP than 6FT at the vessel bottom position near to the T.L. However, in the case of 4PP and MR210, the flow velocity showed almost constant value for MR210 than 4PP.

1.3.3 *Flow pattern*

The flow pattern for 4PP and 6FT are shown in Fig. 11 and 23, respectively. From these flow patterns, it is well observed that both of these impellers produced mainly the axial flow. However, flow velocity is greater for 4PP than 6FT at the vessel bottom position near to the T.L., which was obtained in the previous result. This indicated that a strong axial flow was generated for 4PP than 6FT at this point. Therefore, maximum h distribution is obtained for 4PP.

The flow pattern for 4PP and MR210 are displayed in Fig. 11 and 18, respectively. From these flow patterns, a large circulation flow generated by MR210 is observed to exhibit a more constant h distribution and constant flow velocity thoroughly inside agitated vessels.

In contrary, a strong short pass of axial flow produced by 4PP at the T.L. and vessel bottom position near to the T.L. that provided significant affect to the increases in the intensity of turbulence at the thermal boundary layer. Therefore, h distribution is profoundly increased at these points.

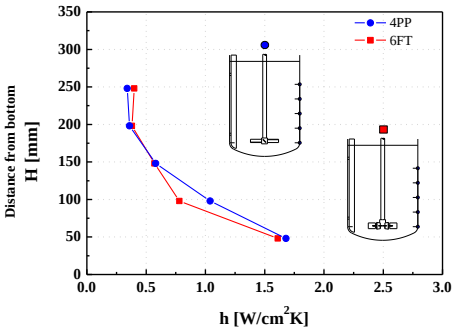

Fig. 19 H vs. h (4PP and 6FT)

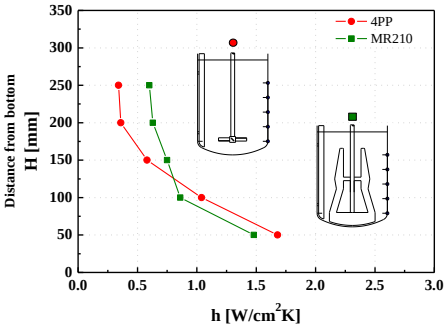

Fig. 20 H vs. h (4PP and MR210)

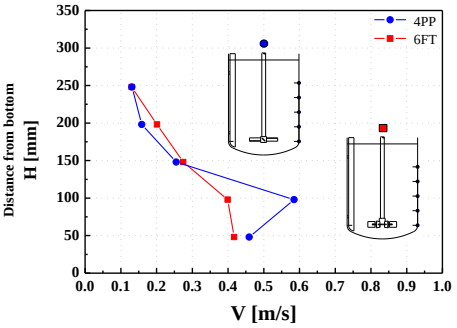

Fig. 21 H vs. h (4PP and 6FT)

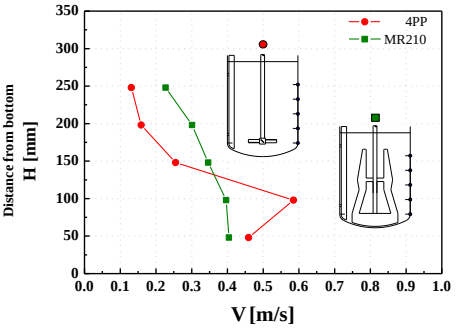

Fig. 22 H vs. V (4PP and MR210)

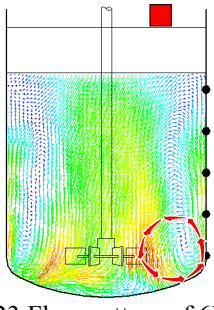

Fig. 23 Flow pattern of 6FT (C/d = 0.5)

2. *Results discussions in non-baffled agitated vessels*

2.1 *The effect of the impeller positions*

2.1.1 *Heat transfer coefficient distribution*

Figs. 24, 25 and 26 show the effect of the impeller positions on the h distribution in the axial direction at the vessel wall in non-baffled agitated vessels for 3P, 4PP and 6FT, respectively. The h distribution shows almost identically for 3P and 4PP, except at the T.L and vessel bottom position near to the T.L. Meanwhile, for 6FT, h distribution is greater at the middle position and vessel bottom position near to the T.L. for the impeller position is located at 1.0.

However, at the impeller position is located at 0.5, maximum h distribution is obtained at the T.L. for 3P, 4PP and 6FT.

2.1.2 *Flow velocity distribution*

Figs. 27, 28 and 29 show the flow velocity for 3P, 4PP and 6FT with the changing of the impeller positions, respectively. From these results obtained, regardless the impeller positions, it is well observed that the flow velocity is almost constant for these impellers. For 3P and 4PP, the flow velocity is slightly greater at the T.L. for the impeller position is located at 0.5 and showed tendency to decrease at the upper position of the vessel.

In contrary, for 6FT, the flow velocity is slightly greater at the middle position and vessel bottom position near to the T.L. and decreased as approaching to the upper position of the vessel when it is located at 0.5.

2.1.3 *Flow pattern visualization*

Figs. 30, 31 and 32 display the close-up flow pattern vicinity to the vessel wall which are positioned at 0.5 for 3P, 4PP and 6FT, respectively. From these flow patterns, it is well observed that upward flow is generated at vicinity to the blades only. In the absence of baffles, the flow created is two dimensional and causing swirling movements as farther away from the blades.

Fig. 33 shows the close-up flow pattern at the vessel bottom for 6FT at the impeller position is located at 0.5. It is clearly observed that a strong axial flow is generated with the flow strikes to the vessel wall with a sharp angle. Hence, maximum h distribution is obtained at this point. Similar flow patterns were also observed for 3P and 4PP.

2.2 *The effect of the impeller speed*

2.2.1 *Heat transfer coefficient distribution*

Figs. 34, 35 and 36 show the effect of the impeller speed on the h distribution for 3P, 4PP and 6FT, respectively. From these results, it is clearly showed that the increases of the impeller speed corresponds to the increased of h distribution.

Furthermore, the h distribution spreads wider as approaching to the T.L. and the maximum h distribution is obtained at this point.

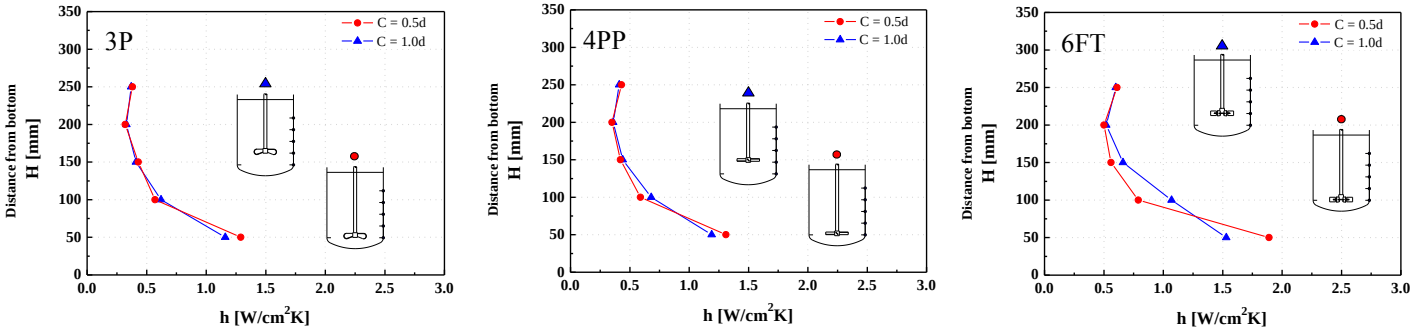

Figs. 24, 25, 26 H vs. h (from left: 3P, 4PP, 6FT) under the effect of the impeller position

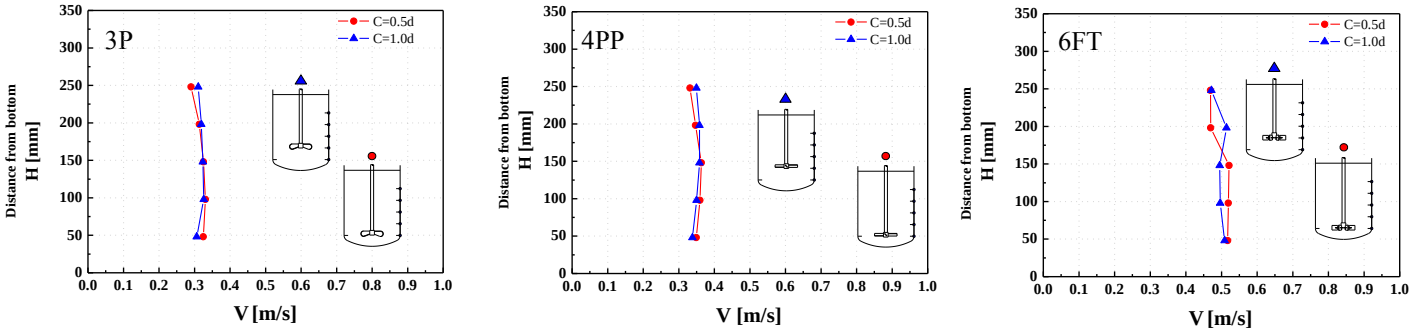

Figs. 27, 28, 29 H vs. V (from left: 3P, 4PP, 6FT) under the effect of the impeller position

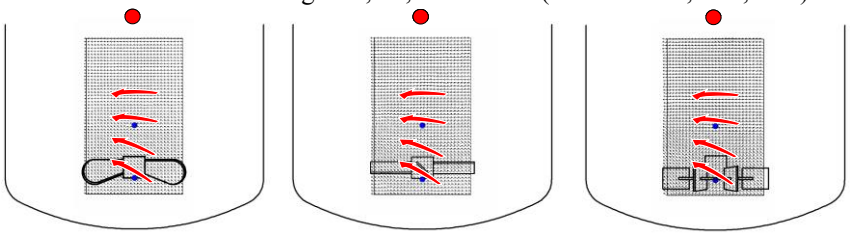

Figs. 30, 31, 32 Flow pattern at the vicinity to the vessel wall (from left: 3P, 4PP, 6FT) (C/d = 0.5)

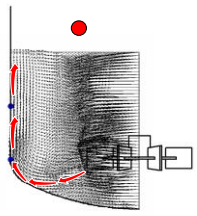

Fig. 33 Flow pattern at the vessel bottom of 6FT (C/d = 0.5)

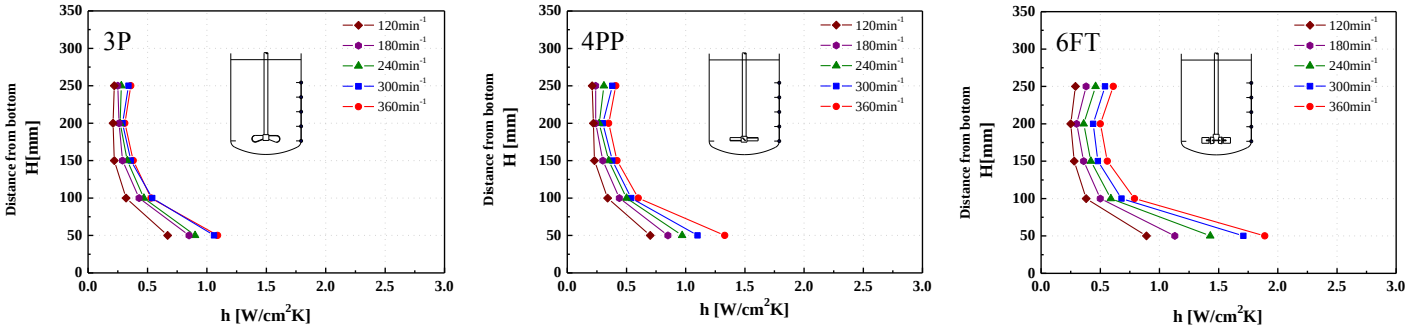

Figs. 34, 35, 36 H vs. h (from left: 3P, 4PP, 6FT) under the effect of the impeller speed

3. *Relationship between the heat transfer distribution and the flow velocity*

Up to here, the effects of the impeller designs, impeller positions and impeller speed on the h distribution inside an agitated vessel were made clear. In order to clarify the relationship between the h distribution and the flow velocity, h distribution is plotted against the flow velocity as shown in Fig. 37. It is made clear that at the T.L., the relationship between the h distribution and the flow velocity get almost a linear line. However, as the clearance between the impeller and the vessel bottom become wider, wide variance were obtained.

This result may give sufficient information for scaling-up works in the future.

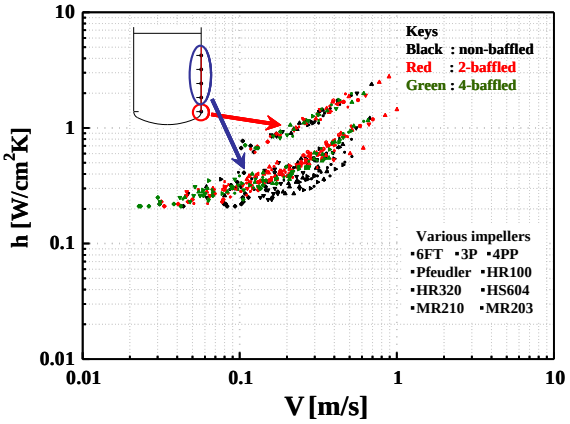

Fig. 37 Relationship between h distribution and flow velocity for various impellers, baffled and non-baffled conditions

CONCLUSIONS

1. Practical data on the h distribution at the inside wall of agitated vessels by using a new measuring method were verified by experimental results.
2. The effects of the impeller design, impeller positions and impeller speed on the h distribution at the inside wall of agitated vessels were made clear.
3. The effects of the flow pattern and the flow velocity were identified to gives greater affect on the h distribution in agitated vessels.

UNITS AND SYMBOLS

C	= clearance between impeller and the vessel bottom	[mm]
D	= diameter of the agitated vessel	[mm]
d	= diameter of impeller	[mm]
H	= distance from the vessel bottom	[mm]
h	= heat transfer coefficient at the inside wall	[W/cm^{2}K]
N	= impeller speed	[min^{-1}]
V	= flow velocity	[m/s]
V_z	= axial velocity	[m/s]
V_θ	= tangential velocity	[m/s]
Pv	= power number per unit volume	[kW/m^3]

REFERENCES

[1] Kanamori, H., Kobayashi, T., Saga, T. and Segawa S., 1990, "Flow Visualization and Analisys of Chemical Agitated Vessel by Particle Imaging Velocimetry," Journal of the Visualization Society of Japan, Vol. 10, No. 2, 239-242

[2] Kuriyama, M., Ohta, M., Yanagawa, K., Arai, K. and Saito, S., 1981, "Heat transfer and temperature distributions in an agitated tank equipped with helical ribbon," Journal of Chemical Engineering of Japan, Vol. 14, No. 4, 323-330

[3] Kobayashi, T., Saga, T., Lee, Y. and Kanamori, H., 1991, "Flow visualization and analysis of 3-D square cavity and mechanically agitated vessels by Particle Imaging Velocimetry," 3rd Triennial International Symposium on Fluid Control, Measurement, and Visualization '91, 401-406

[4] Mitsuishi, N., Miyairi, Y. and Katamine, T., 1973, "Heat transfer to a Newtonian liquids in an agitated vessel," Journal of Chemical Engineering of Japan, Vol. 6, No. 5, 409-414

[5] Mizushina, T., Ito, R., Murakami, Y. and Kiri, M., 1966, "Experimental Study of Newtonian Fluid to the wall of an agitated vessel," Kagaku Kougaku, Vol. 30, No. 8, 719-726

[6] Nagata, S., Nishikawa, M., Takahiro, T., Kida, F. and Kayama, T., 1971, "Jacket Side Heat Transfer Coefficient in Mixing Vessel," Kagaku Kougaku, Vol. 35, No. 8, 924-932